

RESEARCH REPORT

PHOSPHORYLETHANOLAMINE CYTIDYLYLTRANSFERASE 1 modulates flowering in a florigen-independent manner by regulating *SVP*

Hendry Susila, Zeeshan Nasim, Katarzyna Gawarecka, Ji-Yul Jung, Suhyun Jin, Geummin Youn and Ji Hoon Ahn*

ABSTRACT

PHOSPHORYLETHANOLAMINE CYTIDYLYLTRANSFERASE 1 (PECT1) regulates phosphatidylethanolamine biosynthesis and controls the phosphatidylethanolamine:phosphatidylcholine ratio in *Arabidopsis thaliana*. Previous studies have suggested that PECT1 regulates flowering time by modulating the interaction between phosphatidylcholine and FLOWERING LOCUS T (FT), a florigen, in the shoot apical meristem (SAM). Here, we show that knockdown of PECT1 by artificial microRNA in the SAM (*pFD::amiR-PECT1*) accelerated flowering under inductive and even non-inductive conditions, in which FT transcription is almost absent, and in *ft-10 twin sister of ft-1* double mutants under both conditions. Transcriptome analyses suggested that PECT1 affects flowering by regulating SHORT VEGETATIVE PHASE (*SVP*) and GIBBERELLIN 20 OXIDASE 2 (*GA20ox2*). *SVP* misexpression in the SAM suppressed the early flowering of *pFD::amiR-PECT1* plants. *pFD::amiR-PECT1* plants showed increased gibberellin (GA) levels in the SAM, concomitant with the reduction of REPRESSOR OF GA1-3 levels. Consistent with this, GA treatment had little effect on flowering time of *pFD::amiR-PECT1* plants and the GA antagonist paclobutrazol strongly affected flowering in these plants. Together, these results suggest that PECT1 also regulates flowering time through a florigen-independent pathway, modulating *SVP* expression and thus regulating GA production.

KEY WORDS: Flowering, PECT1, *SVP*, *GA20ox2*, Gibberellin, Florigen, *Arabidopsis*

INTRODUCTION

The timing of flowering is precisely regulated by external and internal cues (Andrés and Coupland, 2012). *Arabidopsis thaliana* is a facultative long-day (LD) plant; the LD photoperiod allows the plant to produce sufficient florigen to trigger flowering (Srikanth and Schmid, 2011). In *Arabidopsis*, the florigen is encoded by FLOWERING LOCUS T (*FT*) and its paralogue TWIN SISTER OF FT (*TSF*) (Kardailsky et al., 1999; Kobayashi et al., 1999; Yamaguchi et al., 2005). *FT* and *TSF* transcription is promoted in phloem companion cells in the leaf by CONSTANS (CO), which is a nuclear-localized zinc-finger transcription factor (An et al., 2004; Wenkel et al., 2006). FT and TSF are transported to the shoot apical meristem (SAM), in which they activate the expression of

SUPPRESSOR OF OVEREXPRESSION OF CONSTANS1 (*SOC1*) and *APETALA1* (*API*) and initiate floral primordia development (Andrés and Coupland, 2012; Corbesier et al., 2007).

Under non-inductive short-day (SD) conditions, *Arabidopsis* plants show late flowering (Koornneef et al., 1991). In the light, CO is stabilized by the circadian clock component PSEUDO RESPONSE REGULATOR to promote *FT* and *TSF* transcription; in the dark, CO is degraded by the RING motif-containing E3 ligase CONSTITUTIVE PHOTOMORPHOGENIC 1 (Hayama et al., 2017; Jang et al., 2008; Liu et al., 2008). Therefore, under non-inductive conditions, the low amount of CO limits *FT* and *TSF* expression to levels that are not sufficient to trigger flowering (Takada and Goto, 2003; Yamaguchi et al., 2005).


Flowering under SD conditions is regulated by the gibberellin (GA)- and age-dependent pathways (Srikanth and Schmid, 2011). In the SAM, GA accelerates flowering and floral development by activating the transcription of downstream targets including *LEAFY* (*LFY*), *SOC1*, *FRUITFULL* (*FUL*), *SQUAMOSA PROMOTER BINDING PROTEIN-LIKE 3* (*SPL3*), *SPL5* and *SPL9* (Blázquez et al., 1998; Galvao et al., 2012; Hyun et al., 2016; Moon et al., 2003; Yu et al., 2012). Furthermore, *SPL15* plays an important role downstream of GA in promoting the floral transition under SD conditions through activation of its target genes in cooperation with *SOC1* (Hyun et al., 2016). During the vegetative phase, SHORT VEGETATIVE PHASE (*SVP*) counteracts the effect of GA in promoting flowering (Andrés et al., 2014) by repressing the crucial GA biosynthesis gene *GIBBERELLIN 20 OXIDASE 2* (*GA20ox2*) in the SAM. *SVP* also represses the expression of *SOC1* and *SEPALLATA3* (*SEP3*) to delay flowering (Li et al., 2008; Liu et al., 2009).

FT is a member of the conserved phosphatidylethanolamine binding protein (PEBP) family (Bernier and Jollès, 1984; Serre et al., 1998). FT was suggested to interact with phosphatidylcholine (PC) (Nakamura et al., 2014); PC is generated from phosphoethanolamine, a precursor of phosphatidylethanolamine (PE), and PC levels undergo diurnal oscillations. In *Arabidopsis*, the rate-limiting enzyme PHOSPHORYLETHANOLAMINE CYTIDYLYLTRANSFERASE 1 (PECT1) modulates the PC:PE ratio (Mizoi et al., 2006). Knocking down *PECT1* using artificial microRNA specifically in the SAM (*pFD::amiR-PECT1*) increases PC levels and thus elevates *SOC1* and *API* expression levels, which eventually accelerates flowering time by PC-FT binding (Mizoi et al., 2006; Nakamura et al., 2014). Therefore, it was suggested that the PC-FT interaction in the SAM is important for initiation of flowering by FT (Nakamura et al., 2014). However, the early flowering of *pFD::amiR-PECT1* plants under LD conditions was only partially suppressed in the *ft tsf* mutant background (Nakamura et al., 2014), suggesting that PECT1 also regulates other flowering pathways.

Here, we report a novel role of PECT1 in the regulation of flowering time. PECT1 regulates flowering through transcriptional

Department of Life Sciences, Korea University, Seoul 02841, South Korea.

*Author for correspondence (jahn@korea.ac.kr)

 H.S., 0000-0002-4621-064X; J.H.A., 0000-0003-0347-3922

Handling Editor: Ykä Helariutta
Received 15 June 2020; Accepted 23 November 2020

regulation of the floral repressor *SVP* in the SAM. The *pFD::amiR-PECT1* transgenic lines showed lower expression levels of *SVP* and higher expression levels of its downstream targets *GA20ox2*, *SOC1* and *SEP3*, resulting in early flowering, even under non-inductive conditions such as short photoperiod and low ambient temperature, in which *FT* transcripts are almost absent or present at very low levels. Our results suggested that, in addition to modulating flowering through its effect on PC, *PECT1* also modulates flowering through a florigen-independent pathway via the regulation of *SVP* and *GA20ox2* expression.

RESULTS AND DISCUSSION

SAM-specific knockdown of *PECT1* accelerates flowering independent of florigen

To investigate the role of *PECT1* in flowering time regulation under different environmental conditions, we measured the flowering time of *pFD::amiR-PECT1* plants, in which *PECT1* expression in the SAM is targeted by an artificial miRNA (Nakamura et al., 2014), at 23°C (LD and SD) and 16°C (LD). We confirmed significant downregulation of *PECT1* in the SAM-enriched samples of *pFD::amiR-PECT1* plants, suggesting the lines are suitable for subsequent studies (Fig. S1A).

By counting the total number of leaves at flowering to quantify flowering time, we observed that *pFD::amiR-PECT1* plants flowered earlier than wild-type (WT) Col-0 plants under all conditions tested

(Fig. 1A; Table S1) (Nakamura et al., 2014). In particular, *pFD::amiR-PECT1* plants (lines #2, #4 and #5) flowered earlier than WT under 16°C LD and 23°C SD conditions (Fig. 1A,B), in which the expression levels of *FT* and *TSF* were very low (Fig. S2). Under 23°C SD conditions, WT plants flowered with about 50 leaves, whereas *pFD::amiR-PECT1* lines flowered with 15-17 leaves (Fig. 1A). The ratios of the number of leaves at flowering at different temperatures (16°C/23°C LD) and under different photoperiods (23°C SD/LD) of *pFD::amiR-PECT1* lines #2, #4 and #5 were lower than those of WT plants, indicating that *pFD::amiR-PECT1* plants were temperature- and photoperiod-insensitive (Fig. 1C). Consistent with their accelerated flowering, we observed an increase in the mRNA levels of the floral integrator gene *SOC1* and the floral meristem identity gene *API* in *pFD::amiR-PECT1* lines under 23°C LD and 23°C SD conditions (Fig. S3).

The finding that the *pFD::amiR-PECT1* plants flowered earlier than WT plants under non-inductive conditions raised the possibility that *PECT1* also regulates flowering time in a florigen-independent manner. Therefore, we examined the effect of *pFD::amiR-PECT1* in *ft-10 tsf-1* double mutants, which lack both florigens. Under 23°C LD conditions, *pFD::amiR-PECT1 ft-10 tsf-1* plants flowered earlier than *ft-10 tsf-1* mutants (31.2 ± 1.5 versus 55.8 ± 4.9 leaves; mean \pm s.d.) (Fig. 1D,E; Table S1), consistent with a previous report (Nakamura et al., 2014). In particular, *pFD::amiR-PECT1 ft-10 tsf-1* plants flowered earlier than *ft-10 tsf-1* mutants under 16°C LD (34.0 ± 1.7

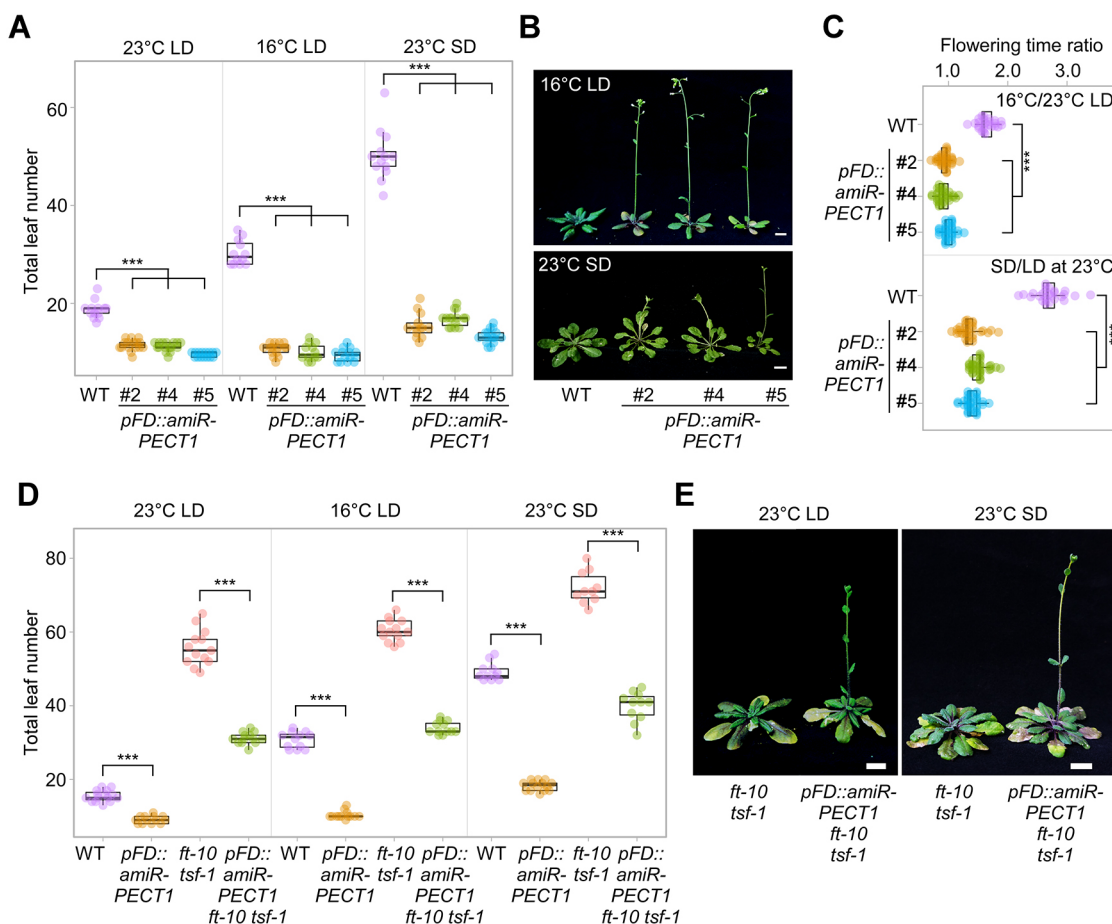


Fig. 1. *pFD::amiR-PECT1* plants showed accelerated flowering in a florigen-independent manner. (A,B) Total leaf number at flowering (A) and morphology (B) of *pFD::amiR-PECT1* plants grown under 23°C LD, 16°C LD and 23°C SD conditions. (C) The leaf number ratio of *pFD::amiR-PECT1* plants under different photoperiods (23°C LD/SD) and temperatures (16°C/23°C LD). (D,E) Total leaf number (D) and morphology (E) of *pFD::amiR-PECT1 ft-10 tsf-1* plants grown under 23°C LD, 16°C LD and 23°C SD conditions. *** $P \leq 0.001$ (two-tailed Student's *t*-tests). Scale bars: 1 cm.

versus 60.5 ± 3.0 leaves) and 23°C SD conditions (39.9 ± 4.0 versus 72.0 ± 4.4 leaves), revealing that acceleration of flowering in *pFD::amiR-PECT1* plants is also independent of *FT* and *TSF*.

RNA-seq analyses identified *SVP* and *GA2ox2* as candidates for the accelerated flowering in *pFD::amiR-PECT1* plants

To identify the genes responsible for accelerated flowering in *pFD::amiR-PECT1* plants in SD, we compared the transcriptome profiles of the SAM-enriched samples of the 10- and 16-day-old *pFD::amiR-PECT1* plants (line #5) grown under 23°C SD conditions (Fig. 2A). RNA-seq analyses showed that the mRNA levels of 652

genes (321 upregulated and 331 downregulated) are affected (≥ 2 -fold and $P \leq 0.01$, Fisher's exact test) by knockdown of *PECT1* in the SAM at day 10, whereas 426 genes (212 upregulated and 214 downregulated) were affected at day 16 (Fig. 2B; Table S2). Among the differentially expressed genes (DEGs), 74 were commonly upregulated and 70 were commonly downregulated (Fig. 2C).

Functional classification of the DEGs in *pFD::amiR-PECT1* plants was performed using Gene Ontology (GO) terms. Fig. S4 lists the top 15 enriched GO-terms of commonly upregulated (Fig. 2D) or downregulated (Fig. 2E) DEGs from both stages. Many commonly upregulated genes were associated with reproductive organ development (shown in blue in Fig. 2D), consistent with the early

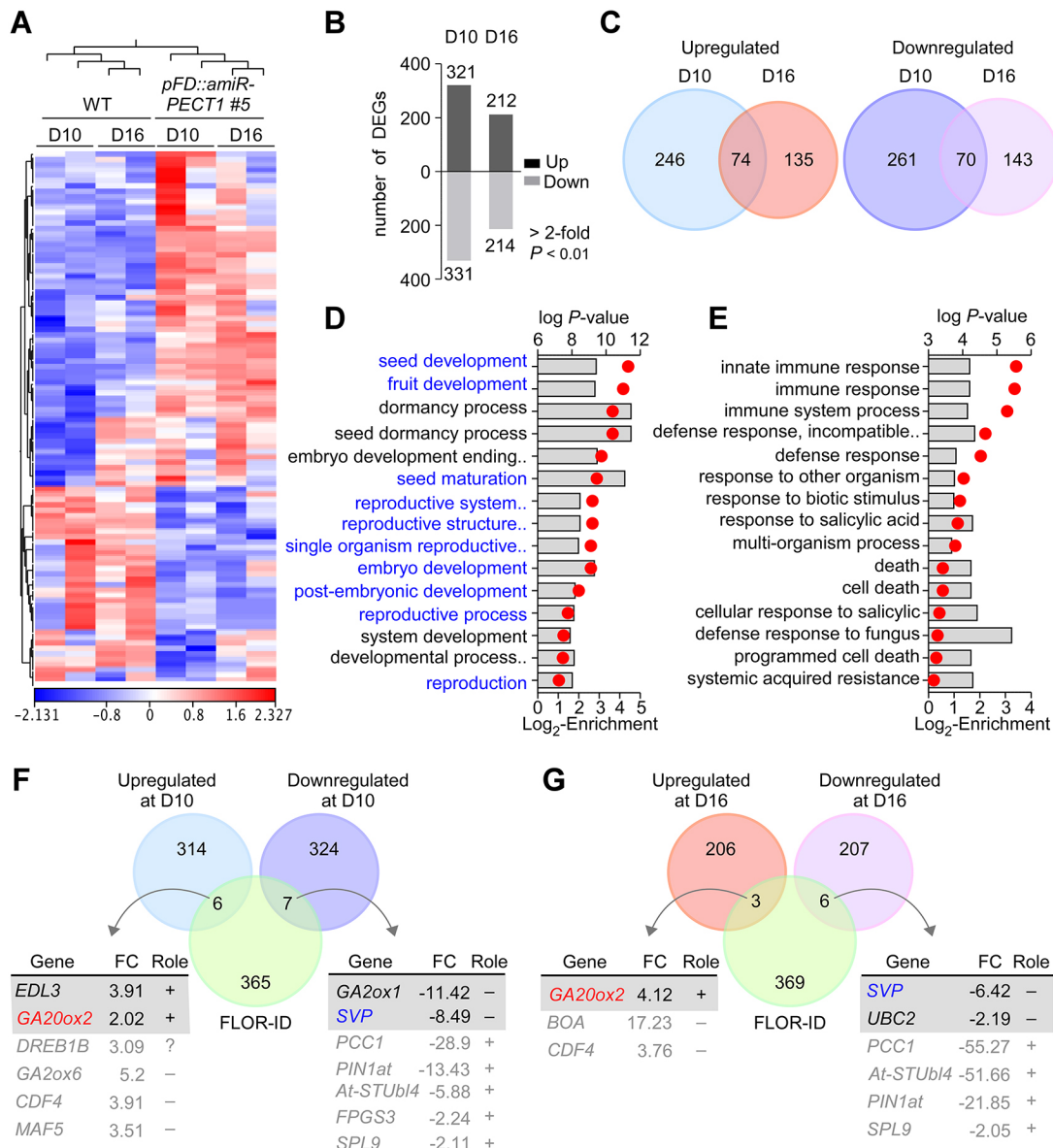


Fig. 2. Differentially expressed genes in the SAM-enriched samples of *pFD::amiR-PECT1* plants. (A) Heatmap of DEGs in 10- and 16-day-old *pFD::amiR-PECT1* plants (line #5) grown under 23°C SD conditions. Samples were harvested at ZT8. Changes in expression levels are represented in a log₂ scale and displayed as colors ranging from blue to red as shown in the key. (B,C) The number of DEGs (>2 -fold, $P \leq 0.01$) (B) and the number of genes commonly upregulated and downregulated (C) in 10- and 16-day-old *pFD::amiR-PECT1* plants. (D,E) Top 15 GO terms enriched among the genes that were commonly upregulated (D) and downregulated (E) in 10- and 16-day-old *pFD::amiR-PECT1* plants. The y-axis represents GO terms; the primary x-axis represents log₂-enrichment (gray bars); the secondary x-axis shows the negative log of P -value (red circles). Blue text highlights the reproductive organ development GO term. (F,G) Venn diagram of the flowering time genes that showed an increase or a decrease in expression levels in the SAM-enriched samples of 10-day-old (F) and 16-day-old (G) *pFD::amiR-PECT1* plants (line #5). FC, fold-change; +, floral promoters; -, floral repressors.

flowering of *pFD::amiR-PECT1* plants under 23°C SD conditions (Fig. S3B). By contrast, many of the commonly downregulated genes in *pFD::amiR-PECT1* plants were related to biotic stimulus, immune response and cell death (Fig. 2E).

To identify the genes responsible for early flowering, we cross-referenced the DEGs with known flowering time genes (FLOR-ID) (Bouche et al., 2016). In 10-day-old *pFD::amiR-PECT1* plants, the levels of 6 and 7 transcripts increased and decreased, respectively, compared with WT (Fig. 2F), and in 16-day-old *pFD::amiR-PECT1* plants, 3 and 6 transcripts increased and decreased, respectively (Fig. 2G). Among the upregulated genes, *GA20ox2* and *CYCLING DOF FACTOR 4 (CDF4)* showed an increase at both stages. However, we excluded *CDF4* from further analyses because it is a floral repressor (Fornara et al., 2009) and its increased expression is inconsistent with the early flowering phenotype of *pFD::amiR-PECT1* plants. By contrast, among the downregulated genes, only *SVP* consistently showed a decrease (8.49- and 6.42-fold) at both stages (Fig. 2F,G).

Therefore, the early flowering of *pFD::amiR-PECT1* plants seen under inductive and non-inductive conditions (Fig. 1A) is probably caused by the downregulation of *SVP* in the SAM, which indirectly elevated *GA20ox2* mRNA levels (Andrés et al., 2014).

PECT1 regulates flowering via SVP and its downstream targets in the SAM

Next, we performed quantitative real-time PCR (qPCR) to confirm the alteration of *SVP* and *GA20ox2* expression. We first prepared different tissues (whole seedlings, leaves and SAM-enriched samples) and validated our sample preparation using *SHOOT MERISTEMLESS (STM)* as the SAM marker and *RUBISCO SMALL SUBUNIT 3B (RBCS3B)* as the leaf marker (Fig. S5). Under 23°C SD conditions, the *SVP* mRNA levels were lower in the SAM-enriched samples of *pFD::amiR-PECT1* lines compared with WT (3.0- to 3.7-fold) (Fig. 3A). A similar decrease (2.1- to 3.0-fold) was seen in whole seedlings, but not in the leaf. Consistent with the qPCR data, *pSVP::GUSplus* expression

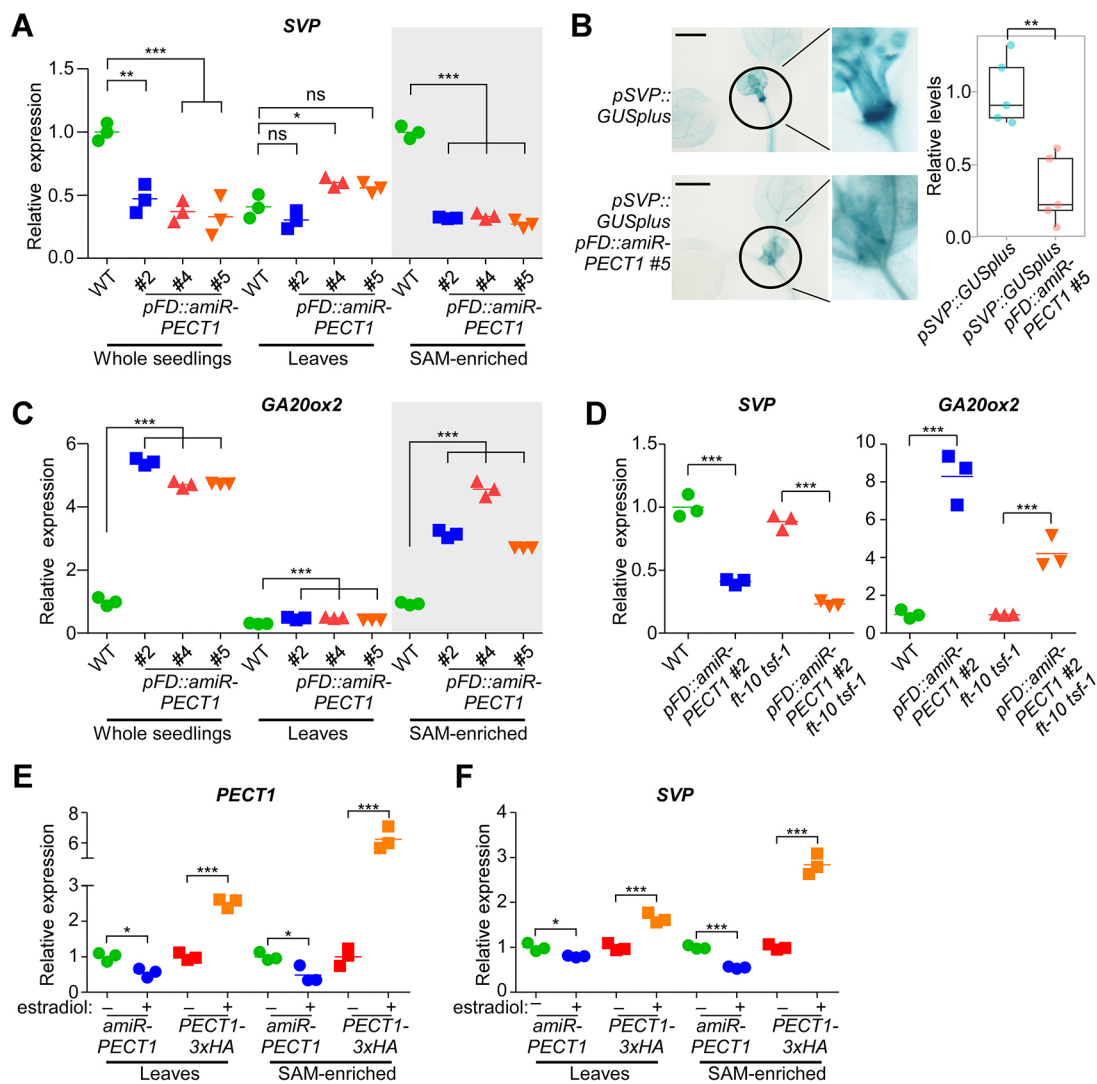


Fig. 3. Early flowering of *pFD::amiR-PECT1* plants is likely regulated through the SVP-gibberellin pathway. (A,C) The mRNA levels of *SVP* (A) and *GA20ox2* (C) in whole seedlings, leaves and SAM-enriched samples of *pFD::amiR-PECT1* plants under 23°C SD conditions (ZT8). (B) GUS staining of the shoot apical region of 10-day-old *pSVP::GUSplus pFD::amiR-PECT1* plants under 23°C SD conditions (ZT8). The graph on the right shows quantification of GUS staining intensity in the shoot apical region. (D) The mRNA levels of *SVP* and *GA20ox2* in *pFD::amiR-PECT1 ft-10 tsf-1* whole seedlings under 23°C SD conditions (ZT8). (E,F) The mRNA levels of *PECT1* (E) and *SVP* (F) in leaves and the SAM-enriched samples of *pER8::amiR-PECT1* and *pER8::PECT1:3xHA* plants under 23°C SD conditions upon estradiol treatment. * $P \leq 0.05$, ** $P \leq 0.01$, *** $P \leq 0.001$ [one-way ANOVA followed by Dunnett's multiple comparisons tests (A,C); two-tailed Student's *t*-test (B,D,E,F)]. ns, non-significant. Scale bars: 2 mm.

in the SAM was lower in *pFD::amiR-PECT1* plants than WT under 23°C SD conditions (Fig. 3B). Concomitant with the downregulation of *SVP*, we observed an increase in mRNA levels of *GA20ox2* (2.9- to 4.9-fold), *SOC1* (1.5- to 1.9-fold) and *SEP3* (7.4- to 12.7-fold), the known downstream targets of *SVP*, in the SAM-enriched samples (Fig. 3C; Fig. S6A,B). Furthermore, the mRNA levels of *LFY*, *FUL* and *SPL3*, GA downstream targets, were also elevated (Fig. S6C,D), suggesting that the GA pathway is activated in *pFD::amiR-PECT1* plants.

Importantly, the expression of *SVP*, *GA20ox2*, *SOC1* and *SEP3* was altered in the *ft-10 tsf-1* background. The *SVP* mRNA levels in *pFD::amiR-PECT1 ft-10 tsf-1* plants were 3.8-fold lower compared with WT, whereas the *GA20ox2*, *SOC1* and *SEP3* mRNA levels were 4.3-, 1.7- and 19.6-fold higher, respectively (Fig. 3D; Fig. S7), consistent with the early flowering of *pFD::amiR-PECT1 ft-10 tsf-1* plants (Fig. 1D,E). This suggested that the altered expression of *SVP*, *GA20ox2*, *SOC1* and *SEP3* was independent of florigens. Under 23°C LD conditions, *SVP* mRNA levels of *pFD::amiR-PECT1* plants were also lower compared with WT, concomitant with higher *GA20ox2* mRNA levels (Fig. S8).

To further elucidate the role of *PECT1*, we expressed *amiR-PECT1* and *PECT1:3×HA* using an estrogen-inducible XVE system (Zuo et al., 2000) (Fig. S9A). The estradiol treatment in the *pER8::amiR-PECT1* plants reduced *PECT1* mRNA levels, whereas it increased *PECT1* mRNA levels in *pER8::PECT1:3×HA* plants (Fig. 3E; Fig. S9B,C). Furthermore, we observed a reduction in *SVP* mRNA levels in *pER8::amiR-PECT1* plants (1.8-fold reduction in the SAM-enriched samples), whereas we observed elevated *SVP* mRNA levels in *pER8::PECT1:3×HA* plants (2.8-fold increase in the SAM-enriched samples) after estradiol treatment (Fig. 3F; Fig. S9D), suggesting that the late flowering of *pFD::PECT1* plants is also due to the elevated levels of *SVP* (Nakamura et al., 2014). A weak alteration in *GA20ox2* and *SEP3* mRNA levels was seen in *pER8::amiR-PECT1* and *pER8::PECT1:3×HA* plants (Fig. S9D,E). These data suggest that *PECT1* acts upstream to regulate *SVP*.

PECT1-mediated flowering is SVP- and GA-dependent

To test the genetic interaction between *PECT1* and *SVP*, we generated *pFD::amiR-PECT1 svp-32* mutants and measured their flowering time at 23°C under LD and SD conditions. No additive acceleration was observed in *pFD::amiR-PECT1 svp-32* plants under 23°C LD conditions (Fig. 4A; Fig. S10A; Table S1) and very weak acceleration of flowering (8.8% decrease in total leaf number) was observed in *pFD::amiR-PECT1 svp-32* mutants only under 23°C SD conditions. The mRNA levels of *GA20ox2*, *SOC1* and *SEP3* were similar in *pFD::amiR-PECT1 svp-32* plants and *svp-32* mutants (Fig. S10B), suggesting that *PECT1* and *SVP* act in the same genetic pathway. Furthermore, expression of *SVP:3×HA* in the SAM driven by the *KNOTTED-LIKE FROM ARABIDOPSIS THALIANA (KNAT1)* promoter (Fig. S11A) partially rescued the early flowering of *pFD::amiR-PECT1* plants under 23°C SD and LD conditions (Fig. 4B; Fig. S11B,C), consistent with the changes in expression levels of *SVP*, *GA20ox2* and *SEP3* in the transgenic lines (Fig. 4C; Fig. S11D).

To confirm whether the alteration of *GA20ox2* mRNA levels in *pFD::amiR-PECT1* plants affected endogenous GA levels, we performed liquid chromatography-mass spectrometry (LC-MS) to quantify the levels of bioactive GAs (GA_3 and GA_4) and the precursors (GA_5) in the SAM-enriched samples. We observed that the levels of all of the tested GAs [both 13-hydroxylated GAs (GA_3 and GA_5) and non-13-hydroxylated GA (GA_4)] were significantly increased (3.9-fold) in *pFD::amiR-PECT1* plants (Fig. 4D), consistent with the increased GA levels of *svp-41* mutants (Andrés

et al., 2014). Consistent with the result, the levels of REPRESSOR OF GA_1-3 (RGA), a DELLA protein (Dill et al., 2001), were reduced in the SAM-enriched samples of *pFD::amiR-PECT1* plants, but not in the leaf (Fig. 4E).

To further examine the involvement of GA, we treated the WT and *pFD::amiR-PECT1* plants with exogenous GA_3 and the GA biosynthesis inhibitor paclobutrazol (PAC) and measured the flowering time under 23°C SD conditions. We confirmed that WT and *pFD::amiR-PECT1* plants responded similarly to GA_3 and PAC treatments by checking the *GA20ox2* mRNA levels (Fig. S12) (Fukazawa et al., 2017). Flowering of *pFD::amiR-PECT1* plants was only slightly accelerated (0.6 to 12.6% reduction in leaf number) by GA_3 treatment, whereas WT plants showed a 40.3% reduction in leaf number (Fig. 4F; Table S1). However, flowering of *pFD::amiR-PECT1* plants was severely delayed upon PAC treatment (64.8 to 70.1% increase in leaf number), whereas WT plants showed a 40.8% increase, suggesting that the accelerated flowering in *pFD::amiR-PECT1* plants was associated with increased GA levels (Fig. 4D). Nevertheless, flowering of PAC-treated *pFD::amiR-PECT1* plants was still earlier than PAC-treated WT plants, suggesting that GA is not the only factor involved in the regulation of flowering time by *PECT1*, as *SOC1* and *SEP3* were also upregulated in *pFD::amiR-PECT1* plants (Fig. S6A,B).

In summary, our study identified another novel pathway for flowering time regulation by *PECT1*. In addition to the mechanism shown in Nakamura et al. (2014), our results revealed that the effect of *PECT1* on flowering time is also through the modulation of *SVP* expression and its downstream targets (*GA20ox2*, *SOC1* and *SEP3*) (Fig. 4G). The methylation of PE during PE:PC biosynthesis affects histone methylation status, which in turn modulates gene expression in yeasts and human cells (Ye et al., 2017), suggesting that membrane phospholipids and histones are closely linked in cell metabolism; however, further research is required to test this possibility in plants.

MATERIALS AND METHODS

Plant materials, growth conditions, chemical treatments and flowering time measurement

The mutants used in this study are in the Columbia (Col) background. *pFD::amiR-PECT1*, *pFD::amiR-PECT1 ft-10 tsf-1*, *ft-10 tsf-1*, and *svp-32* have been described previously (Lee et al., 2007; Nakamura et al., 2014; Yamaguchi et al., 2005). The *pFD::amiR-PECT1* lines were kindly provided by Prof. George Coupland (The Max Planck Institute for Plant Breeding Research, Germany). The *pFD::amiR-PECT1 ft-10 tsf-1* mutants were kindly provided by Prof. Yuki Nakamura (Institute of Plant and Microbial Biology, Academia Sinica, Taiwan). Plants were grown in soil or on half-strength Murashige and Skoog (MS) media at 16°C or 23°C under LD (16 h:8 h light:dark) and at 23°C under SD (8 h:16 h light:dark) conditions. For chemical treatments, β -estradiol (estradiol) (Sigma-Aldrich), GA_3 (Duchefa Biochimie) and PAC (Sigma-Aldrich) stock solutions were prepared in DMSO. Mock (DMSO) and 100 μ M estradiol were prepared in water and added on the top of MS medium containing 8-day-old plants, which were incubated under 23°C SD conditions for 2 days. For flowering time measurement, mock (DMSO), 50 μ M GA_3 and 5 μ M PAC were prepared in water and applied by irrigation twice a week until flowering. The total leaf number was counted when the primary inflorescence reached ~5 cm. Box plots were constructed to represent flowering time distribution (Postma and Goedhart, 2019). The data are summarized as a boxplot, with the box indicating the interquartile range (IQR), the whiskers showing the range of values that are within 1.5× IQR and a horizontal line indicating the median.

Plasmid construction

To generate *pSVP::GUSplus* transgenic plants, the promoter region of *SVP* was cloned into *pENTR2B::GUSplus* entry vector using In-Fusion cloning method (Clontech). The fused *pSVP::GUSplus* fragment was then cloned into

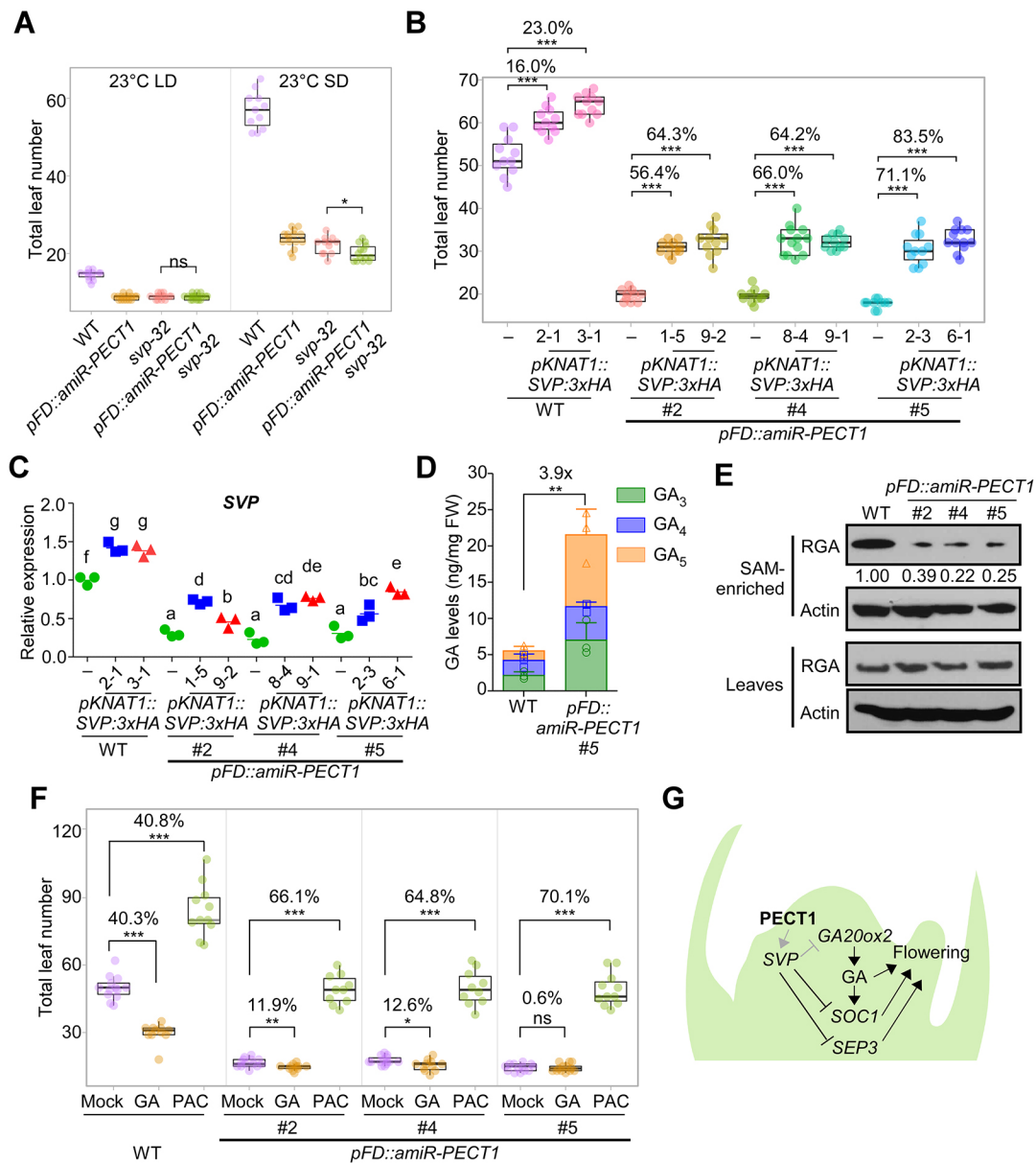


Fig. 4. *PECT1* delays flowering time through *SVP* and *GA*. (A) Total leaf number at flowering of *pFD::amiR-PECT1 svp-32* mutants at 23°C under LD and SD conditions. (B,C) Total leaf number at flowering (B) and *SVP* mRNA levels in the SAM-enriched samples (C) of *pKNAT1::SVP:3xHA pFD::amiR-PECT1* plants under 23°C SD conditions. (D,E) Quantification of *GA* levels in the 10-day-old SAM-enriched samples of *pFD::amiR-PECT1* plants (D) and *RGA* protein levels (E) in the *pFD::amiR-PECT1* plants under 23°C SD conditions (ZT8). *RGA* levels in the WT were set to 1. (F) Total leaf number of *pFD::amiR-PECT1* plants grown on soil supplemented with *GA*₃ or paclobutrazol (PAC) under 23°C SD conditions. (G) A working model of *PECT1* function in flowering. *PECT1* indirectly activates *SVP* expression, thus inhibiting the expression of *GA20ox2*, *SEP3* and *SOC1* to prevent precocious flowering. Black and gray lines represent direct and indirect regulation, respectively. * $P < 0.05$, ** $P < 0.01$, *** $P < 0.001$ (two-tailed Student's *t*-tests). In C, different lowercase letters represent groups that are statistically significantly different from one another derived from one-way ANOVA followed by Duncan's multiple range tests ($P < 0.01$). ns, non-significant.

the binary vector pEarleyGate 304 (Earley et al., 2006) using the Gateway cloning system (Invitrogen). To generate *pKNAT1::SVP:3xHA*, the coding sequence of *SVP* was cloned into 3×*HA*-containing entry vector (Wang et al., 2013). The fused *SVP:3xHA* fragment was then cloned into modified *pJHA212G* binary vector containing *Nopaline Synthase* terminator (*NosT*) and the *KNAT1* promoter (Yoo et al., 2005) using the Gateway cloning system. To generate *pER8::amiR-PECT1*, *pER8::PECT1:3xHA* and *pER-GUS* constructs, the respective sequences were cloned into the entry vector *pENTR2B* for *amiR-PECT1* and *GUS*, and *PECT1* was cloned into an entry vector containing 3×*HA* (Wang et al., 2013). The resulting chimeric sequences were then cloned into the *pER8* vector using the Gateway cloning system. Information on the primers used for amplification is given in Table S3.

Gene expression analyses

For mRNA analyses, total RNA was extracted from plant tissues using Plant RNA Purification Reagent (Invitrogen), and RNA was used as a template for cDNA synthesis using the M-MLV RT, RNaseH⁻ (ElpisBio). The transcript levels were measured by qPCR using a QuantStudio5 qPCR instrument (Applied Biosystems). For normalization, two stably expressed genes, *PP2A3* (*AT1G13320*) and a *SAND* family protein (*AT2G29390*) were used (Hong et al., 2010). For validation assays, sampling was done at zeitgeber time (ZT) 8 for 23°C SD conditions and ZT16 for 23°C LD conditions. All qPCR experiments were carried out in three biological replicates, each with three technical replicates. Primers for qPCR (Table S3) were designed according to previously suggested criteria (Die and Roman, 2012). The relative abundance of transcripts was

calculated according to the geNorm using the PCR efficiency and the Ct values (Hong et al., 2010).

For protein analyses, total protein was extracted from the seedlings using ProPrep Protein Extraction Buffer (iNtRON Biotechnologies). Proteins were separated by SDS-PAGE and transferred to Immobilon-P PVDF membranes (Millipore Corporation). Anti-HA high affinity monoclonal antibodies (clone 3F10, Sigma-Aldrich, 1:5000), anti-RGA polyclonal antibodies (AS11 1630, Agrisera, 1:1000) and anti-Actin polyclonal antibodies (AS13 2640, Agrisera, 1:10,000) were used as primary antibodies, with anti-rat (A9037, Sigma-Aldrich, 1:10,000) or anti-rabbit HRP-conjugated secondary antibodies (A6154, Sigma-Aldrich, 1:10,000 for anti-RGA and 1:20,000 for anti-Actin).

RNA-seq and bioinformatics analyses

RNA was isolated from SAM-enriched samples, which were collected from the shoot apical region of at least 20-25 plants, of the WT and *pFD::amiR-PECT1* plants (line #5). The libraries were constructed using NEBNext Ultra II Directional RNA-seq kit (New England Biolabs) and sequenced using the Illumina HiSeq X Ten platform. The resulting fastq files (GSE147212) were checked for quality using FastQC and then the reads were aligned to TAIR10 reference genome. DEGs were identified using CLC genomics Workbench v.11 as the genes with at least 2-fold change and a *P*-value smaller than 0.01. For GO analysis, Plaza 3.0 (Proost et al., 2015) was used.

GUS staining assays

GUS staining was performed as previously described (Jefferson et al., 1987). The *pSVP::GUSplus* and *pSVP::GUSplus pFD::amiR-PECT1* seedlings were grown at 23°C under SD conditions. Plant samples, pre-treated with 90% acetone, were soaked in X-Gluc solution and incubated at 37°C. Chlorophyll was removed in ethanol at 60°C, and samples were visualized using an Axioskop 2 plus microscope (Zeiss).

GA quantification

GA levels were quantified using 10-day-old SAM-enriched samples of *pFD::amiR-PECT1* plants grown on MS media under 23°C SD conditions (ZT8). Experiments were performed using three biological replicates. GA extraction and quantification was performed as previously described (Li et al., 2017) without a derivatization procedure, using a 6460 Triple quadrupole mass spectrometer (QQQ) comprised of a 1200 series HPLC system at Korea Basic Science Institute (KBSI). A Chemcobond 5-ODS-H (50×2.1 mm, 5 μm) (ChemcoPak) was used with an oven (40°C). GA₃ (Sigma-Aldrich), GA₄, GA₅ and deuterium isotope-labeled GA₄ ([17-2H₂]-GA₄) (Olchemim) were used as standard. The monitoring conditions for all of the tested GA and the internal standard are listed in Table S4.

Acknowledgements

We thank Prof. George Coupland (Max Planck Institute for Plant Breeding Research, Germany) and Prof. Yuki Nakamura (Institute of Plant and Microbial Biology, Academia Sinica, Taiwan) for kindly providing research materials. We thank Jae Kwan Kim, Hocheol Hwang and Hyewon Jeong for their technical assistance.

Competing interests

The authors declare no competing or financial interests.

Author contributions

Conceptualization: H.S., J.H.A.; Methodology: H.S.; Software: Z.N.; Formal analysis: H.S., S.J., G.Y.; Investigation: H.S., K.G., J.-Y.J.; Writing - original draft: H.S., J.H.A.; Writing - review & editing: H.S., Z.N., J.H.A.; Supervision: H.S., J.H.A.; Project administration: J.H.A.; Funding acquisition: J.H.A.

Funding

This work was supported by a National Research Foundation of Korea grant funded by the Korean government (NRF-2017R1A2B3009624 to J.H.A.) and Samsung Science and Technology Foundation (SSTF-BA1602-12 to J.H.A.).

Data availability

The raw RNA-sequencing data are available at NCBI under accession number GSE147212.

Supplementary information

Supplementary information available online at <https://dev.biologists.org/lookup/doi/10.1242/dev.193870.supplemental>

References

- An, H., Roussot, C., Suárez-López, P., Corbesier, L., Vincent, C., Piñeiro, M., Hepworth, S., Mouradov, A., Justin, S., Turnbull, C. et al. (2004). CONSTANS acts in the phloem to regulate a systemic signal that induces photoperiodic flowering of *Arabidopsis*. *Development* **131**, 3615-3626. doi:10.1242/dev.01231
- Andrés, F. and Coupland, G. (2012). The genetic basis of flowering responses to seasonal cues. *Nat. Rev. Genet.* **13**, 627-639. doi:10.1038/nrg3291
- Andrés, F., Porri, A., Torti, S., Mateos, J., Romera-Branchat, M., García-Martínez, J. L., Fornara, F., Gregis, V., Kater, M. M. and Coupland, G. (2014). SHORT VEGETATIVE PHASE reduces gibberellin biosynthesis at the *Arabidopsis* shoot apex to regulate the floral transition. *Proc. Natl. Acad. Sci. USA* **111**, E2760-E2769. doi:10.1073/pnas.1409567111
- Bernier, I. and Jollès, P. (1984). Purification and characterization of a basic 23 kDa cytosolic protein from bovine brain. *Biochim. Biophys. Acta (BBA) - Protein Struct. Mol. Enzymol.* **790**, 174-181. doi:10.1016/0167-4838(84)90221-8
- Blázquez, M. A., Green, R., Nilsson, O., Sussman, M. R. and Weigel, D. (1998). Gibberellins promote flowering of *Arabidopsis* by activating the *LEAFY* promoter. *Plant Cell* **10**, 791-800. doi:10.1105/tpc.10.5.791
- Bouché, F., Lobet, G., Tocquin, P. and Périlleux, C. (2016). FLOR-ID: an interactive database of flowering-time gene networks in *Arabidopsis thaliana*. *Nucleic Acids Res.* **44**, D1167-D1171. doi:10.1093/nar/gkv1054
- Corbesier, L., Vincent, C., Jang, S., Fornara, F., Fan, Q., Searle, I., Giakountis, A., Farrona, S., Gissot, L., Turnbull, C. et al. (2007). FT protein movement contributes to long-distance signaling in floral induction of *Arabidopsis*. *Science* **316**, 1030-1033. doi:10.1126/science.1141752
- Die, J. V. and Roman, B. (2012). RNA quality assessment: a view from plant qPCR studies. *J. Exp. Bot.* **63**, 6069-6077. doi:10.1093/jxb/ers276
- Dill, A., Jung, H.-S. and Sun, T.-P. (2001). The DELLA motif is essential for gibberellin-induced degradation of RGA. *Proc. Natl. Acad. Sci. USA* **98**, 14162-14167. doi:10.1073/pnas.251534098
- Earley, K. W., Haag, J. R., Pontes, O., Opper, K., Juehne, T., Song, K. and Pikaard, C. S. (2006). Gateway-compatible vectors for plant functional genomics and proteomics. *Plant J.* **45**, 616-629. doi:10.1111/j.1365-313X.2005.02617.x
- Fornara, F., Panigrahi, K. C. S., Gissot, L., Sauerbrunn, N., Rühl, M., Jarillo, J. A. and Coupland, G. (2009). *Arabidopsis* DOF transcription factors act redundantly to reduce CONSTANS expression and are essential for a photoperiodic flowering response. *Dev. Cell* **17**, 75-86. doi:10.1016/j.devcel.2009.06.015
- Fukazawa, J., Mori, M., Watanabe, S., Miyamoto, C., Ito, T. and Takahashi, Y. (2017). DELLA-GAF1 complex is a main component in gibberellin feedback regulation of GA20 oxidase 2. *Plant Physiol.* **175**, 1395-1406. doi:10.1104/pp.17.00282
- Galvao, V. C., Horrer, D., Kuttner, F. and Schmid, M. (2012). Spatial control of flowering by DELLA proteins in *Arabidopsis thaliana*. *Development* **139**, 4072-4082. doi:10.1242/dev.080879
- Hayama, R., Sarid-Krebs, L., Richter, R., Fernández, V., Jang, S. and Coupland, G. (2017). PSEUDO RESPONSE REGULATORS stabilize CONSTANS protein to promote flowering in response to day length. *EMBO J.* **36**, 904-918. doi:10.15252/embj.201693907
- Hong, S. M., Bahn, S. C., Lyu, A., Jung, H. S. and Ahn, J. H. (2010). Identification and testing of superior reference genes for a starting pool of transcript normalization in *Arabidopsis*. *Plant Cell Physiol.* **51**, 1694-1706. doi:10.1093/pcp/pcq128
- Hyun, Y., Richter, R., Vincent, C., Martínez-Gallegos, R., Porri, A. and Coupland, G. (2016). Multi-layered regulation of SPL15 and cooperation with SOC1 integrate endogenous flowering pathways at the *Arabidopsis* shoot meristem. *Dev. Cell* **37**, 254-266. doi:10.1016/j.devcel.2016.04.001
- Jang, S., Marchal, V., Panigrahi, K. C. S., Wenkel, S., Soppe, W., Deng, X.-W., Valverde, F. and Coupland, G. (2008). *Arabidopsis* COP1 shapes the temporal pattern of CO accumulation conferring a photoperiodic flowering response. *EMBO J.* **27**, 1277-1288. doi:10.1038/emboj.2008.68
- Jefferson, R. A., Kavanagh, T. A. and Bevan, M. W. (1987). GUS fusions: beta-glucuronidase as a sensitive and versatile gene fusion marker in higher plants. *EMBO J.* **6**, 3901-3907. doi:10.1002/j.1460-2075.1987.tb02730.x
- Kardailsky, I., Shukla, V. K., Ahn, J. H., Dagenais, N., Christensen, S. K., Nguyen, J. T., Chory, J., Harrison, M. J. and Weigel, D. (1999). Activation tagging of the floral inducer FT. *Science* **286**, 1962-1965. doi:10.1126/science.286.5446.1962
- Kobayashi, Y., Kaya, H., Goto, K., Iwabuchi, M. and Araki, T. (1999). A pair of related genes with antagonistic roles in mediating flowering signals. *Science* **286**, 1960-1962. doi:10.1126/science.286.5446.1960
- Koornneef, M., Hanhart, C. J. and van der Veen, J. H. (1991). A genetic and physiological analysis of late flowering mutants in *Arabidopsis thaliana*. *Mol. Gen. Genet.* **229**, 57-66. doi:10.1007/BF00264213

- Lee, J. H., Yoo, S. J., Park, S. H., Hwang, I., Lee, J. S. and Ahn, J. H. (2007). Role of SVP in the control of flowering time by ambient temperature in Arabidopsis. *Genes Dev.* **21**, 397-402. doi:10.1101/gad.1518407
- Li, D., Liu, C., Shen, L., Wu, Y., Chen, H., Robertson, M., Helliwell, C. A., Ito, T., Meyerowitz, E. and Yu, H. (2008). A repressor complex governs the integration of flowering signals in Arabidopsis. *Dev. Cell* **15**, 110-120. doi:10.1016/j.devcel.2008.05.002
- Li, D., Guo, Z., Liu, C., Li, J., Xu, W. and Chen, Y. (2017). Quantification of near-atomole gibberellins in floral organs dissected from a single Arabidopsis thaliana flower. *Plant J.* **91**, 547-557. doi:10.1111/tpj.13580
- Liu, L.-J., Zhang, Y.-C., Li, Q.-H., Sang, Y., Mao, J., Lian, H.-L., Wang, L. and Yang, H.-Q. (2008). COP1-mediated ubiquitination of CONSTANS is implicated in Cryptochrome regulation of flowering in Arabidopsis. *Plant Cell* **20**, 292-306. doi:10.1105/tpc.107.057281
- Liu, C., Xi, W., Shen, L., Tan, C. and Yu, H. (2009). Regulation of floral patterning by flowering time genes. *Dev. Cell* **16**, 711-722. doi:10.1016/j.devcel.2009.03.011
- Mizoi, J., Nakamura, M. and Nishida, I. (2006). Defects in CTP: PHOSPHORYLETHANOLAMINE CYTIDYLTRANSFERASE affect embryonic and postembryonic development in Arabidopsis. *Plant Cell* **18**, 3370-3385. doi:10.1105/tpc.106.040840
- Moon, J., Suh, S.-S., Lee, H., Choi, K.-R., Hong, C. B., Paek, N.-C., Kim, S.-G. and Lee, I. (2003). The SOC1 MADS-box gene integrates vernalization and gibberellin signals for flowering in Arabidopsis. *Plant J.* **35**, 613-623. doi:10.1046/j.1365-313X.2003.01833.x
- Nakamura, Y., Andrés, F., Kanehara, K., Liu, Y.-c., Dörmann, P. and Coupland, G. (2014). Arabidopsis florigen FT binds to diurnally oscillating phospholipids that accelerate flowering. *Nat. Commun.* **5**, 3553. doi:10.1038/ncomms4553
- Postma, M. and Goedhart, J. (2019). PlotsOfData—A web app for visualizing data together with their summaries. *PLoS Biol.* **17**, e3000202. doi:10.1371/journal.pbio.3000202
- Proost, S., Van Bel, M., Vanechoutte, D., Van de Peer, Y., Inzé, D., Mueller-Roeber, B. and Vandepoele, K. (2015). PLAZA 3.0: an access point for plant comparative genomics. *Nucleic Acids Res.* **43**, D974-D981. doi:10.1093/nar/iku986
- Serre, L., Vallée, B., Bureaud, N., Schoentgen, F. and Zelwer, C. (1998). Crystal structure of the phosphatidylethanolamine-binding protein from bovine brain: a novel structural class of phospholipid-binding proteins. *Structure* **6**, 1255-1265. doi:10.1016/S0969-2126(98)00126-9
- Srikanth, A. and Schmid, M. (2011). Regulation of flowering time: all roads lead to Rome. *Cell. Mol. Life Sci.* **68**, 2013-2037. doi:10.1007/s00018-011-0673-y
- Takada, S. and Goto, K. (2003). TERMINAL FLOWER2, an Arabidopsis Homolog of HETEROCHROMATIN PROTEIN1, Counteracts the activation of FLOWERING LOCUS T by CONSTANS in the vascular tissues of leaves to regulate flowering time. *Plant Cell* **15**, 2856-2865. doi:10.1105/tpc.016345
- Wang, X., Fan, C., Zhang, X., Zhu, J. and Fu, Y.-F. (2013). BioVector, a flexible system for gene specific-expression in plants. *BMC Plant Biol.* **13**, 198. doi:10.1186/1471-2229-13-198
- Wenkel, S., Turck, F., Singer, K., Gissot, L., Le Gourrierc, J., Samach, A. and Coupland, G. (2006). CONSTANS and the CCAAT box binding complex share a functionally important domain and interact to regulate flowering of Arabidopsis. *Plant Cell* **18**, 2971-2984. doi:10.1105/tpc.106.043299
- Yamaguchi, A., Kobayashi, Y., Goto, K., Abe, M. and Araki, T. (2005). TWIN SISTER OF FT (TSF) acts as a floral pathway integrator redundantly with FT. *Plant Cell Physiol.* **46**, 1175-1189. doi:10.1093/pccp/pci151
- Ye, C., Sutter, B. M., Wang, Y., Kuang, Z. and Tu, B. P. (2017). A metabolic function for Phospholipid and histone methylation. *Mol. Cell* **66**, 180-193.e8. doi:10.1016/j.molcel.2017.02.026
- Yoo, S. Y., Bomblies, K., Yoo, S. K., Yang, J. W., Choi, M. S., Lee, J. S., Weigel, D. and Ahn, J. H. (2005). The 35S promoter used in a selectable marker gene of a plant transformation vector affects the expression of the transgene. *Planta* **221**, 523-530. doi:10.1007/s00425-004-1466-4
- Yu, S., Galvão, V. C., Zhang, Y.-C., Horrer, D., Zhang, T.-Q., Hao, Y.-H., Feng, Y.-Q., Wang, S., Schmid, M. and Wang, J.-W. (2012). Gibberellin regulates the Arabidopsis floral transition through miR156-targeted SQUAMOSA PROMOTER BINDING-LIKE transcription factors. *Plant Cell* **24**, 3320-3332. doi:10.1105/tpc.112.101014
- Zuo, J., Niu, Q.-W. and Chua, N.-H. (2000). An estrogen receptor-based transactivator XVE mediates highly inducible gene expression in transgenic plants. *Plant J.* **24**, 265-273. doi:10.1046/j.1365-313x.2000.00868.x